Zeitschrift: Helvetica Physica Acta
Band: 43 (1970)
Heft: 4

Artikel: The decay of 51Cr
Autor: Ribordy, Cl. / Huber, O.
DOI: https://doi.org/10.5169/seals-114175

The Decay of ^{51}Cr [1])

by **Cl. Ribordy** [2]) and **O. Huber**

Institut de Physique de l'Université de Fribourg (Suisse)

(16. II. 70)

Abstract. The decay of ^{51}Cr is studied with a Ge(Li) detector of 3.2 cm^3 and a double focusing beta spectrometer. Hypothetical transitions (150 keV, 325 keV, 470 keV and 645 keV) in ^{51}V are excluded. The energy and K-internal conversion coefficient of the single γ-transition in ^{51}V are measured: $E_\gamma = (320.032 \pm 0.040)$ keV and $\alpha_K = (1.46 \pm 0.13) \times 10^{-3}$. The Q value of the decay $^{51}Cr \rightarrow {}^{51}V$ is obtained from the end point energy of the internal bremsstrahlung (IB) spectrum: $Q = (748 \pm 14)$ keV. This IB spectrum is measured with a Ge(Li) detector and unfolded with a described procedure. Although a pile up rejector was used, this Ge(Li) measurement suffers still from a distortion due to the pile up effect. The IB spectrum taken with the magnetic spectrometer (Pile up free) reveals a deformation which remains unclear. The proportion of the electron captures populating the first excited state of ^{51}V is measured: $\beta = (10.2 \pm 1)\,\%$. A decay scheme is proposed.

1. Introduction

Some authors [1–3] have previously proposed in ^{51}V a $3/2+$ level at 645 keV [2] weakly populated by the electron capture decay of ^{51}Cr (Fig. 1). The basic configuration of ^{51}V being $(f\,7/2)^3$, the shell model with a strong jj-coupling [4, 5] predicts for this configuration the spin sequence $7/2-$ (ground state), $5/2-$, $3/2-$, $11/2-$, $9/2-$ and $15/2-$, which has been confirmed experimentally [6].

More recently Scholz [7] using the strong coupling symmetric rotator model has developped a level scheme. Excepted for the 1st excited state ($5/2-$), the level positions are better predicted than by the shell model, although the spin sequence is identical.

Both models predict the negative parity for all the low energy levels. Therefore the existence of a positive parity state between first (320 keV) and second (928 keV) excited states would cause a theoretical problem.

Such an even state would most probably result from a $(f\,7/2)^4$ configuration plus a proton hole in one of the lower closed shells. But according to Schwäger [6], this configuration seems to create a series of states between 2.7 and 3.4 MeV. This energy interval lies considerably higher than 645 keV.

[1]) Work supported by the Fonds National Suisse de la Recherche Scientifique.

[2]) Present adress: Département de Physique, Faculté des Sciences, Université Laval, Québec (P.Q.), Canada.

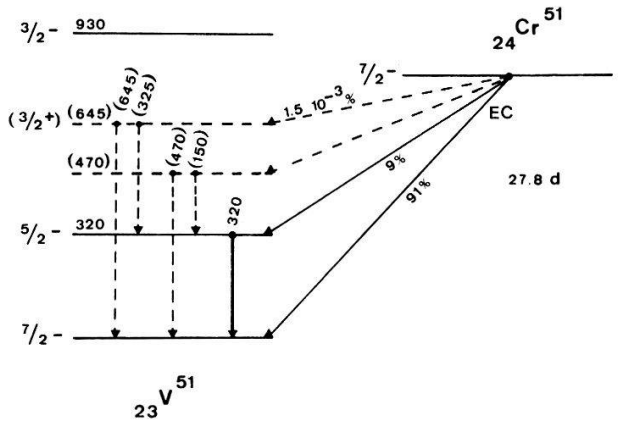

Figure 1
The decay scheme of ^{51}Cr. (Derived from Ofer [2] and Mathé [3].) The weakly populated levels at (645) and (470) keV and their corresponding crossover and stopover transitions proposed by Ofer [2] resp. Mathé [3] will be excluded by this paper. Our proposed decay scheme is presented in Figure 10.

Moreover Bisi [1] and Ofer [2] measured for this 3/2+ level at 645 keV population rates which differ by a factor 50.

Three further weak transitions (470), (325), (150) keV (Fig. 1) have been mentionned in ^{51}V [2–3].

All of these 4 transitions have been announced from scintillation measurements, where the pile up effect is difficult to suppress. As we shall see in section (2.3) two peaks at 645 keV and 470 keV may result from this pile up effect. The existence of the levels at 645 keV and 470 keV becomes somewhat doubtful. Therefore we investigated these weak transitions with a double focusing $\pi\sqrt{2}$ spectrometer [8] (Pile up impossible) and a Ge(Li) detector of 3.2 cm^3, where the resolution is good enough to distinguish between photopeaks and pile up features.

2. Hypothetical Transitions in ^{51}V

2.1 (645) *keV transition*[3])

The existence of a level at 645 keV was postulated mainly from the measurement of his ground state transition [1–3].

Therefore, using the method of external conversion in the magnetic spectrometer, we looked for a 645 keV K-conversion line. Figure 2 represents between 600 and 660 keV the internal bremsstrahlung spectrum emitted by the electron capture transition leading to ground state of ^{51}V. No conversion line at all can be seen.

We can assign an upper limit to the intensity of a contingent line in this energy region. We define as limit of detection, a line the amplitude of which equals twice the standard deviation of the experimental points of the ground spectrum: such a pseudo-line is drawn on Figure 2 at 645 K.

The comparison of this line to the strong 320 K line (Ground state transition from the first excited level) yields an upper limit for the intensity of a possible 645 keV transition: 1.0×10^{-6} per disintegration. We can extend this limit to the whole energy region of Figure 2 (600–660 keV). This limit is 90 times lower than the one we deduced from a previous measurement [9].

[3]) The parentheses mean that the mentionned transition is hypothetical.

Table 1
Intensities (per 10^6 dis.) of the hypothetical transitions in ^{51}V

Ref.	Instrument	(150) keV	(325) keV		(470) keV	(645) keV	
		Intensity	Energy	Intensity	Intensity	Energy	Intensity
Bisi [1]	NaI(Tl)	–	–	–	–	624	(260 ± 30)
Ofer [2]	NaI(Tl)	–	–	–	–	645	5
Ofer [2]	NaI(Tl)–NaI(Tl) coinc	–	320 ± 20	10	–	–	–
Bunker [13]	NaI(Tl)	–	–	–	< 400	–	–
Mathé [3]	NaI(Tl)	–	–	–	–	630	(10 ± 4)
Mathé [3]	NaI(Tl)–NaI(Tl) coinc	exists	320	exists	(3 ± 2)	–	–
Kern [9]	Magn sp	–	–	–	–	624	< 90
Ribordy [10]	Ge(Li)	–	–	–	< 2.4	–	–
Kluk [11]	NaI(Tl)	–	–	–	< 1.4	640	< 0.95
Hill [12]	Ge(Li)–NaI(Tl) coinc	< 0.44	315–325	< 10	< 1.6	–	–
Hill [12]	Ge(Li)	–	300	< 2.2	–	635–645	< 2.5
Hill [12]	Ge(Li)	–	–	–	–	630	< 1.0
Present work	Magn sp	–	–	–	–	600–660	< 1.0
	Ge(Li)	–	325–340	< 1.4	< 0.5	–	–

Table 2
The K-ICC for the 320.0 keV transition in ^{51}V

Ref.	Method	α_K, α_T	Multipolarity
Maeder [30]	NaI(Tl)	1.5 × 10^{-3}	M1
Bunker [31]	Magn lens IC[a]), calib. with α_K of 411.8 keV (^{198}Au)	α_T = (1.62 ± 0.16) × 10^{-3}	–
Bunker [31]	Calculation α_T^{exp}, $K/L + M + \ldots$ theoretical	α_K = (1.47 ± 0.2) × 10^{-3}	M1 + 13% E2
Estulin [32]	Proportional counter	(2.9 ± 0.2) × 10^{-3}	E2
O'Friel [33]	Magn lens IEC[b])	(1.5 ± 0.2) × 10^{-3}	M1
O'Friel [34]	Magn lens IEC[b])	(1.38 ± 0.13) × 10^{-3}	M1
Gupta [35]	CsI(Tl), Plastic scint	(1.6 ± 0.2) × 10^{-3}	–
Present work	IEC Magn sp	(1.46 ± 0.13) × 10^{-3}	M1 + (11.7 ± 4) % E2

[a]) Internal conversion. [b]) Internal and external conversion.

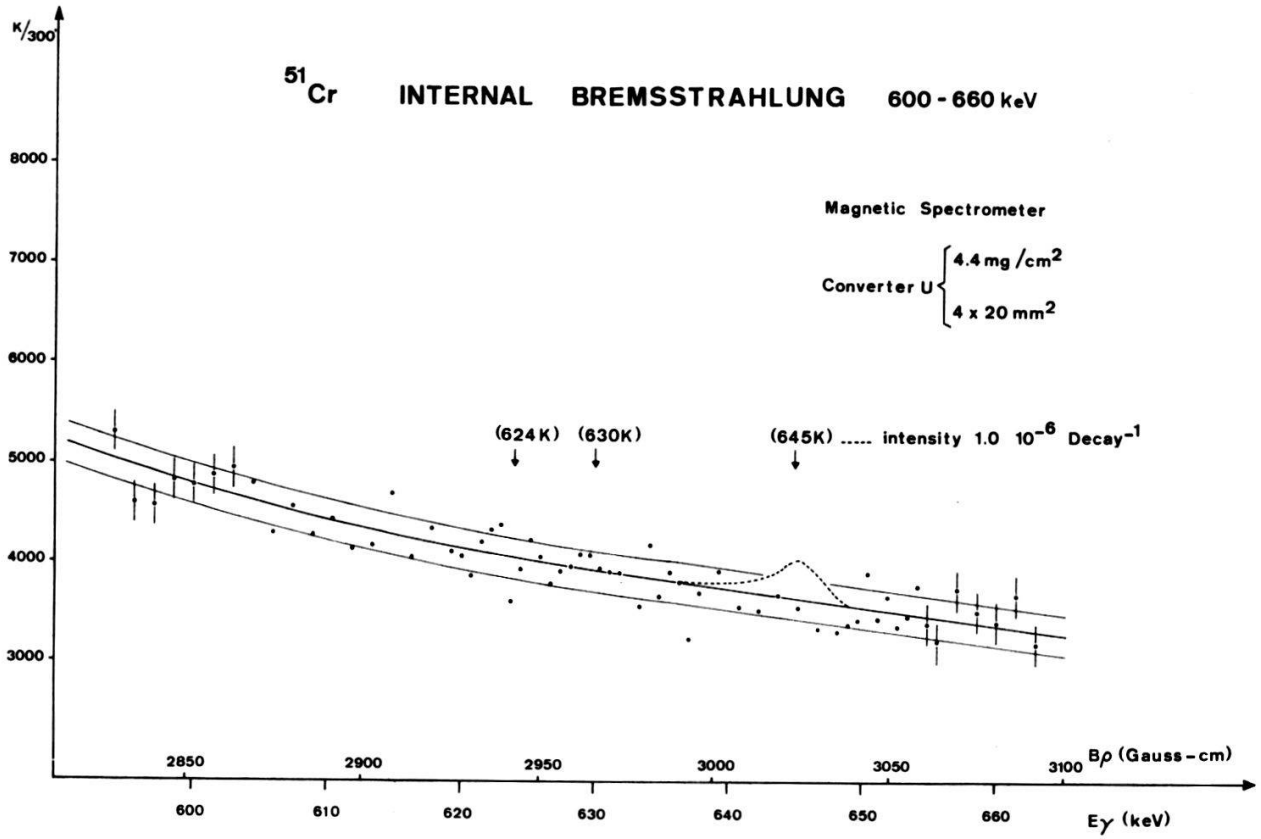

Figure 2

The internal bremsstrahlung spectrum from the electron capture ^{51}Cr 7/2- $\rightarrow$ ^{51}V 7/2-measured in external conversion. The upper- and under-line define the $\pm\,\sigma$ band around the spectrum curve. The dotted line represents a pseudo K-conversion line which would attest a γ-transition with the intensity 1.0×10^{-6} decay^{-1}. The E_γ-scale defines the γ-energy which causes a K-conversion at the B_ϱ-value of the upper scale.

The Table 1 compares our result with other measurements. Bisi [1], Ofer [2] and Mathé [3] found a line at 624 respectively 645 and 630 keV with an intensity 260 respectively 5 and 10 times higher than our limit which has been confirmed by further authors [11, 12].

2.2 (150) *keV*, (325) *keV and* (470) *keV transitions*

Similar measurements yielded intensity upper limits for these transitions. Table 1 compares these upper limits with the previous intensity values.

2.3 *Discussion*

The (645) and (470) keV lines as measured by Bisi and Ofer respectively Mathé result surely from a pile up effect. Actually the prominent features of the mono-energetic spectrum resulting from the strong 320 keV transition are the photopeak and the group composed by the Compton edge and the backscattering peak at 150 keV (Fig. 3).

The probability of pile up is then largest at 470 and 640 keV. Our pile up rejector (Fig. 4) has a finite resolving time (50 ns) which is 100 times shorter than the pulse length. The pile up of pulses which are coincident within this resolving time cannot be rejected. Therefore a deformation still remains at 470 and 640 keV.

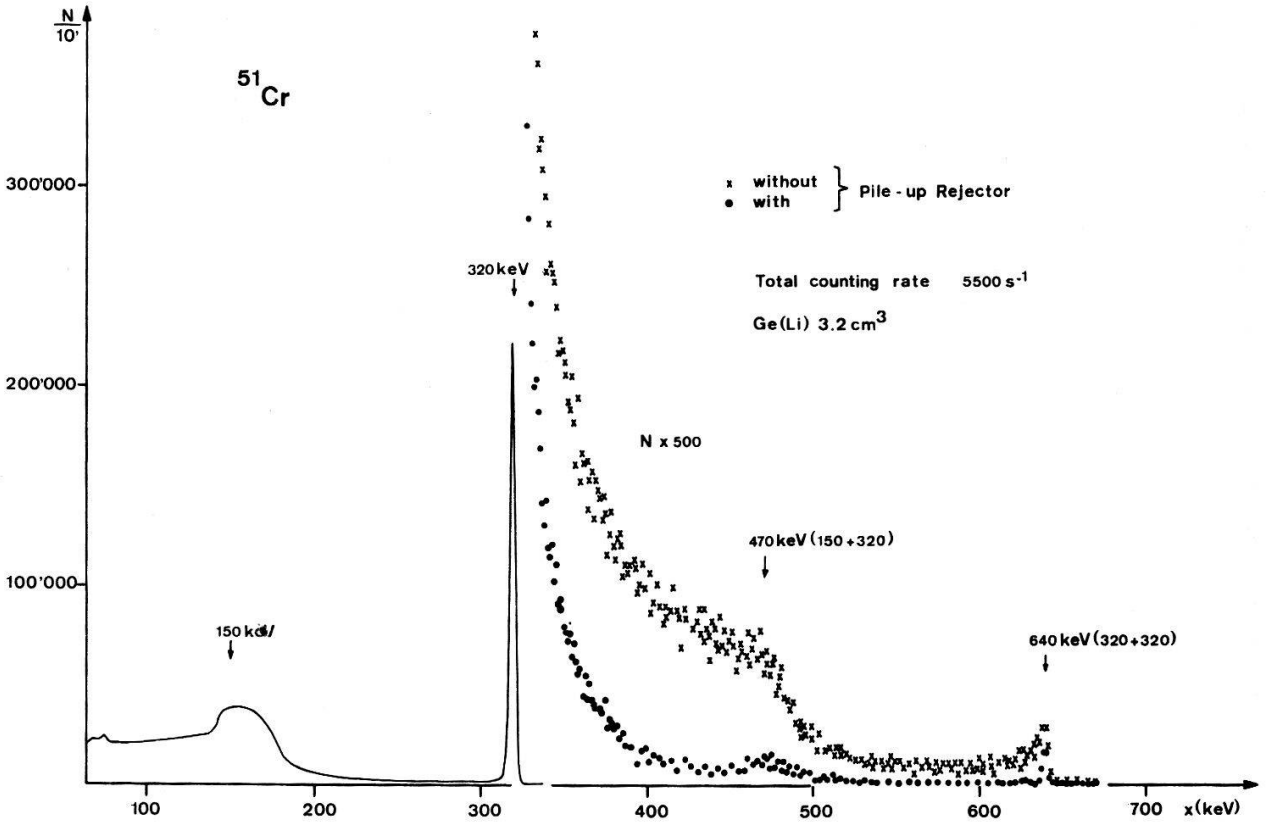

Figure 3
The γ-spectrum (Ge(Li)) from the decay of ^{51}Cr. The right part shows the high energy portion of the internal bremsstrahlung spectrum measured with and without a pile up rejector.

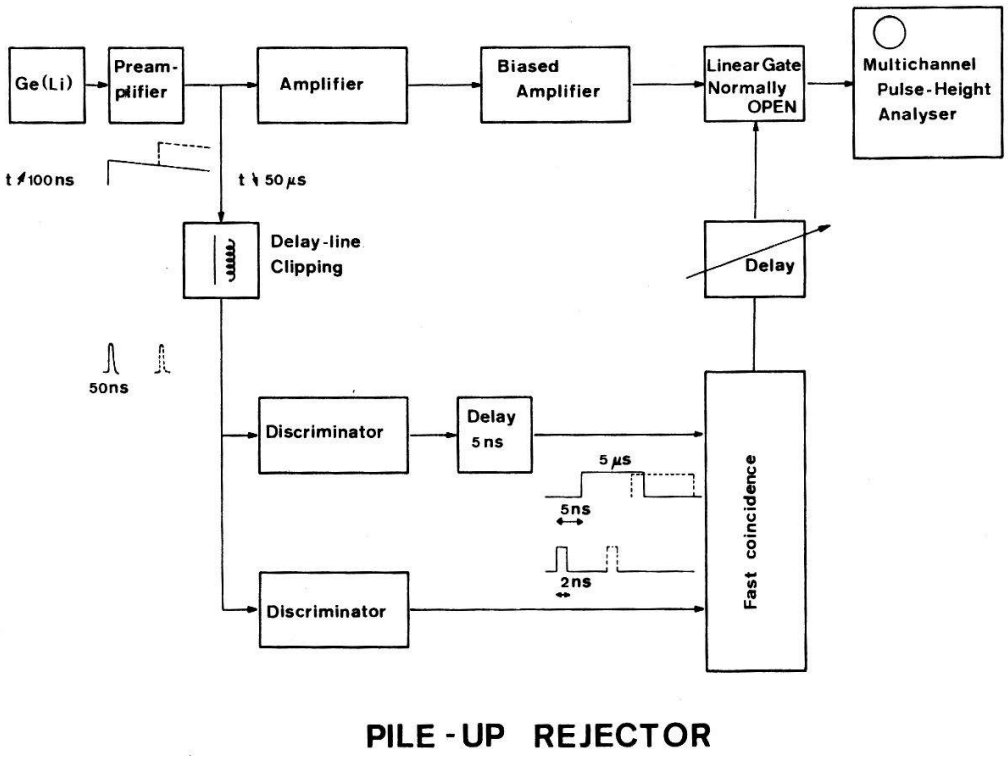

Figure 4
Blockscheme of the pile up rejector used for the measurements shown in Figures 3 and 5. The resolving time was 50 ns.

The resolution of the scintillation detectors was poor enough to lead Bisi, Ofer and Mathé to identify the broad features at 150 and 470 keV as photopeaks. This is no more possible in a Ge(Li) spectrum. Consequently the (150) keV and (470) keV transitions proposed by Mathé do not exist.

Our spectrum taken in external conversion (Fig. 2) enables us to exclude the (645) keV peak observed by Bisi, Ofer and Mathé.

The measurement of a (645) keV transition has suggested to Ofer and Mathé the possible existence of the (325) keV transition which is now excluded.

If nevertheless some of the above mentionned transitions would exist, their intensities would be inferior to the lowest limit given for each of them on Table 1.

As the 2 levels at 470 and 645 keV do not exist, the ^{51}Cr emits a monoenergetic γ-radiation, what is very useful for calibration. In this purpose we measured precisely the 320 keV transition (Energy and K-internal conversion coefficient) and the Q value of the decay.

3. 320 keV Transition

3.1 *Transition energy*

We measured the K-external conversion line with our magnetic double-focusing spectrometer. We used the following geometry:

Converter: { Uranium, 1.06 mg/cm^2 ; 2×20 mm^2

Resolution: $2.6^0/_{00}$

Calibration: ^{192}Ir [14] { 295.938 $\pm$ 0.009 keV ; 308.429 $\pm$ 0.010 keV ; 316.486 $\pm$ 0.010 keV ; 468.053 $\pm$ 0.014 keV

As the importance of the low energy tail varies with the energy, the centroid of the line is not reproducible with enough accuracy. Therefore the position of the line was best defined as the abscissa of the point situated on the high energy edge at half maximum.

The calibration straight line was obtained by a linear least squares technique. We obtained after 10 measurements an average value for the transition energy:

$$\boxed{E_\gamma = (320.032 \pm 0.040)\ \text{keV}}\ .$$

The given error is the standard deviation. This value is compatible with the previous values listed on Table 3. Let us discuss the energy value of Reidy [20].

For the energy of the transitions emitted in the decay of ^{140}La, Kern [21] pointed out discrepancies with the results of Baer et al. [22], but found a good agreement with the values of Gunnink et al. [23]. The values of Baer are always larger and the difference increases with the energy, what points to a systematic error. Baer and Reidy [20] used the same instrument. Reidy's result agrees better with ours, if we subtract from it the amount of this difference (23 eV).

3.2 *K-internal conversion coefficient (K-ICC)*

We measured the K-internal conversion coefficient α_K with the so-called 'internal external conversion' method developped by Hultberg [24, 25]. α_K is derived from the intensity ratio A_K/A_γ of the recorded external and K-internal conversion lines:

$$\alpha_K = \frac{A_K}{A_\gamma} f \tau_K \frac{k_\gamma}{k_\beta} b\, d\,.$$

A_K, A_γ	intensities of the internal resp. external K-conversion lines
f	f (Source-converter geometry, E_γ) [25, 26]
τ_K	K-shell photoelectric cross-section (barns/atom) [27]
d	converter foil thickness (mg/cm^2)
k_β, k_γ	strengths (sec^{-1}) of the sources used for the internal resp. external conversion measurements
b	dimension factor $= 6.025/M\ 10^{-4}$ atom cm^2/barns mg
M	atomic weight of the converter element

Hultberg calculated the f factor for our source-converter geometry. We used an Au converter, the thickness of which was (1.588 ± 0.010) mg/cm^2. After 10 measurements with the momentum resolution 1.8 $^0/_{00}$ we obtained the average value:

$$\boxed{\alpha_K = (1.46 \pm 0.13) \times 10^{-3}}\,.$$

The K-ICC for pure M1 and E2 multipolarity are extrapolated [28] from the directly calculated ICC of Rose [29] ($Z = 25, 35, 45, 55$):

Multipolarity	α_K
M1	1.12×10^{-3}
E2	4.03×10^{-3}

From these ICC we determine a M1 + (11.7 ± 4)% E2 mixture for this 320.0 keV transition. There is agreement with all previous values (Table 2) except with the value of Estulin.

Table 3
The energy of the 320 keV transition in ^{51}V

Ref.	Instrument	Energy (keV)
Kern [9]	Magn sp ext conv	320.0 ± 0.2
Ewan [15]	Ge(Li)	320.3 ± 0.3
Robinson [16]	Ge(Li)	319.8 ± 0.3
Pierson [17]	NaI(Tl)	320.28 ± 0.66
White [18]	Bent crist sp	320.18 ± 0.21
Black [19]	Ge(Li)	320.07 ± 0.05
Reidy [20]	Bent crist sp	320.085 ± 0.006
Present work	Magn sp ext conv	320.032 ± 0.040

4. The Q Value and the Spectrum of Internal Bremsstrahlung (IB)

4.1 *The IB measurement*

The Q value of the decay $^{51}Cr \rightarrow {}^{51}V$ can be obtained from the threshold energy of the inverse reaction $^{51}V(p, n)^{51}Cr$ [36] or from the end point energy W_0 of the IB spectrum emitted by the electron capture transition leading to the ground state of ^{51}V:

$$Q = W_0 + B \tag{4.1.1}$$

B is the binding energy of the captured electron. We measured the IB spectrum with a Ge(Li) detector of 3.2 cm³ (Fig. 5). In order to reduce as much as possible the distortion of this spectrum by the pile up effect, we used the above mentionned pile up rejector and measured with a low total counting rate ($\sim 400\ s^{-1}$) during 85 hours. The spectrum was registered in a 512 channel analyser RCL.

This measured spectrum has to be corrected for several factors like background, Compton contribution, finite resolution and the gamma-efficiency of the detector. The second and the third corrections were performed by an unfolding procedure (Sections 4.2 and 4.3). The efficiency curve has been determined with an accuracy of 3%. The end point energy W_0 is then available from the so-called 'JAUCH plot' which is computed from the corrected spectrum (Section 4.4).

4.2 *The unfolding procedure*

Our measured spectrum consists of n numbers[4]) N_i. Each of them represents the amount of events in our γ-ray spectrometer with an energy value between[5]) $x_0 + (i-1)\,\Delta x$ and $x_0 + i\,\Delta x$. The amount N_i results not only from photoelectrical events created in this ith x-channel but also from Compton events caused by photons of higher energies. Then $\boldsymbol{N}$ is not a true picture of the real γ-spectrum[6]) $\boldsymbol{S}$ and therefore cannot be compared directly to the theoretical spectral shape (Section 4.4).

In order to find a mathematical relationship between $\boldsymbol{S}$ and $\boldsymbol{N}$, we define the quantity a^*_{ij} as the probability for one γ-ray, the energy E_j of which corresponds to the jth E-channel to cause an event in the ith x-channel. These a^*_{ij} compose an array $\boldsymbol{A^*}$, the so-called *response matrix* of the γ-ray spectrometer. Each of its columns has the shape of a single spectrum the photopeak of which is positionned on the diagonal element. Each of these spectra may be considered as a function of x with E as parameter (Fig. 6):

$$a^*_{ij} = a^*(x_i, E_j)\ . \tag{4.2.1}$$

We may now express each number N_i as the sum of the contributions in the ith x-channel of S_j photons E_j:

$$\sum_{j=1}^{n} a^*_{ij}\, S_j = N_i \qquad (i = 1, 2, \ldots, n)\ . \tag{4.2.2}$$

[4]) We get together these n numbers under a vector $\boldsymbol{N}$. The index i refers to the ith channel of the spectrometer scale (x-channel).

[5]) x_0 = zero-energy, Δx = channel width.

[6]) i.e. n numbers S_j. The index j refers to the jth channel of the γ-energy scale (E-channel). The x and E-scale are independent but have the same energy calibration.

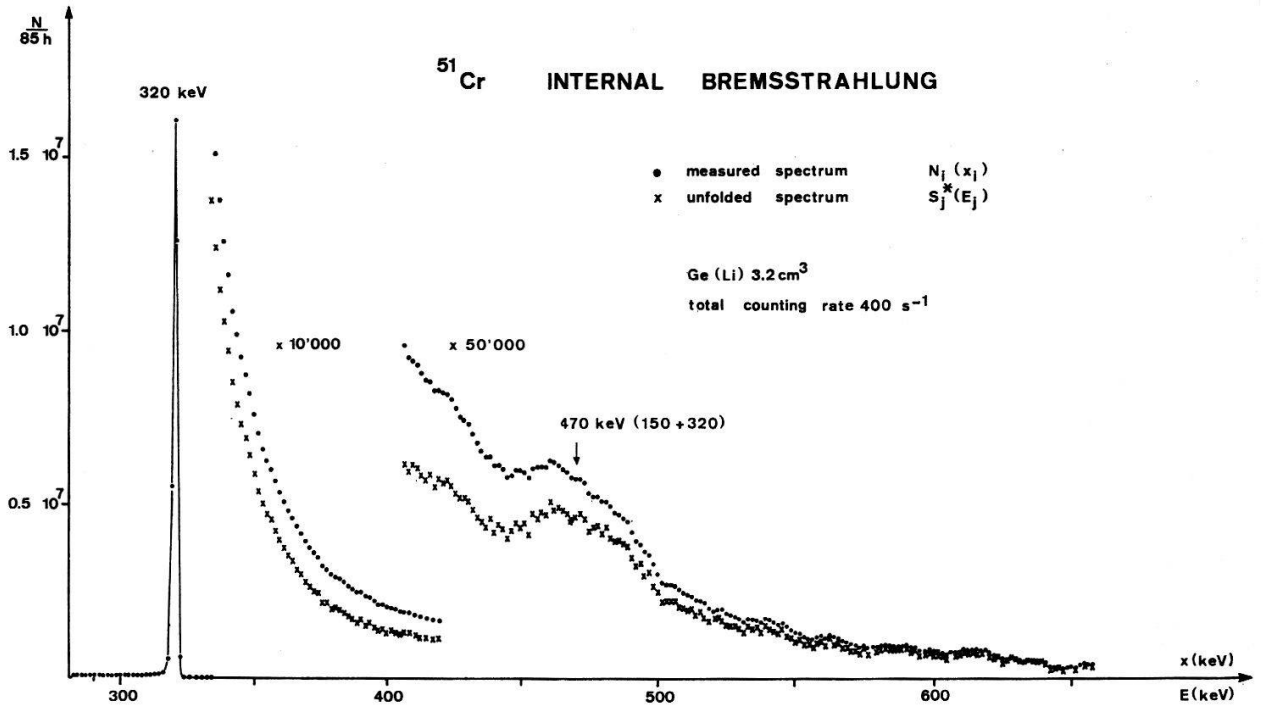

Figure 5

The IB spectrum measured with the analysing system shown at Figure 4. The background spectrum and the pile up peak at 640 keV are already subtracted. The deformation at 470 keV is caused by the pile up of 2 events of 320 keV and 150 keV (Fig. 3). The (x) represent the spectrum resulting from the unfolding procedure described by section (4.2).

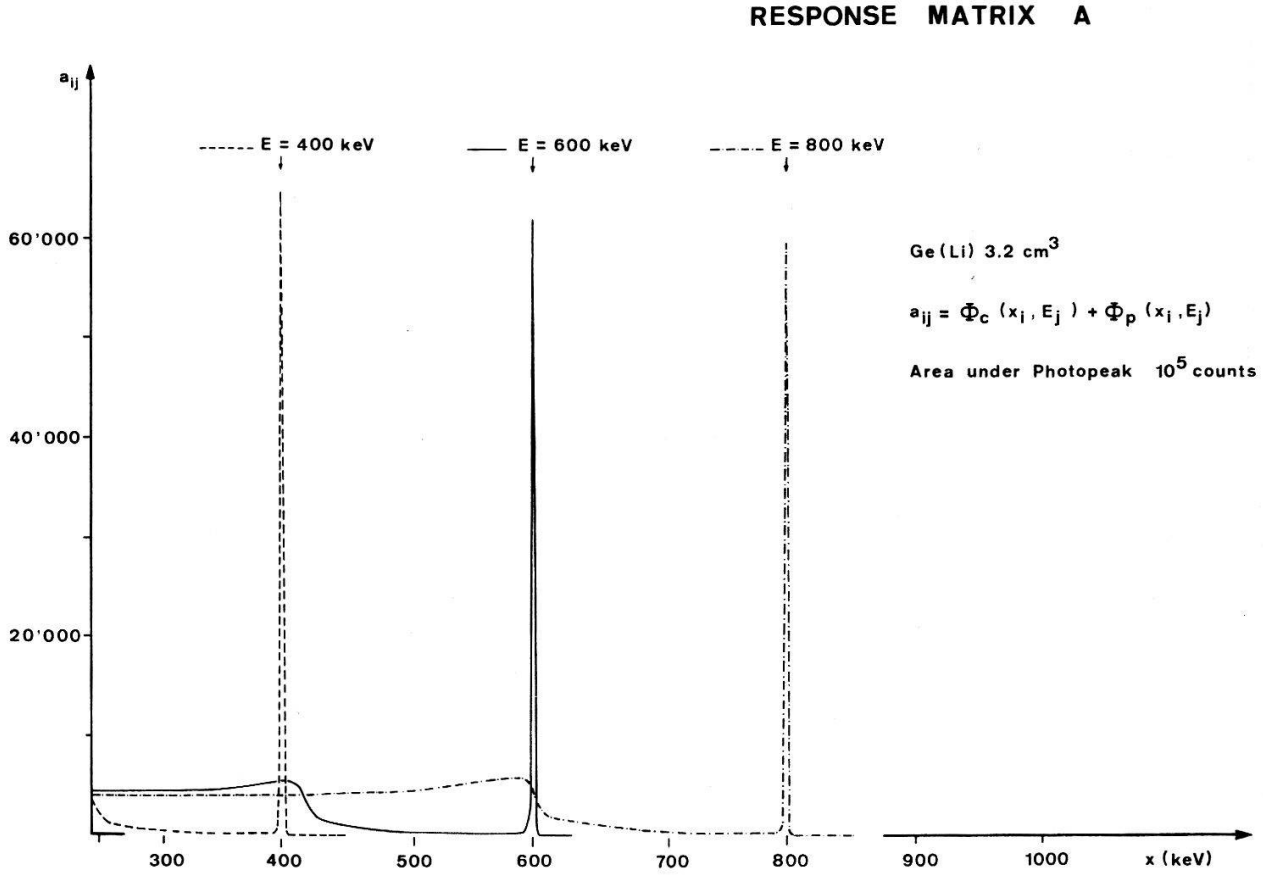

Figure 6

Three single γ-spectra computed to construct the response matrix $\boldsymbol{A}$ of the γ-ray detector used for the IB measurement shown in Figure 5.

The real γ-spectrum $\boldsymbol{S}$ may be calculated from the measured spectrum $\boldsymbol{N}$ by solving the system (4.2.2). This procedure is called the *unfolding* of the spectrum $\boldsymbol{N}$.

According to the definition of $\boldsymbol{A}^*$ each single spectrum is so normalized that its total integral equals unity. This requirement is not suitable, because it supposes the knowledge of the Compton distribution up to energies approaching zero, which we do not need, our first x-channel being set at 280 keV.

We renormalize the matrix $\boldsymbol{A}^*$ in a more practical way so that the area of the photopeak on each column is unity.

The section (4.3) describes the construction of the single spectra composing the columns of the new response matrix $\boldsymbol{A}$. Three of them ($E = 400$,600 and 800 keV) are shown in Figure 6.

The total efficiency of the γ-ray detector is no more included in $\boldsymbol{A}$ but only the photo-to-Compton ratio is conserved therein. If we use this new matrix, we get the following system:

$$\sum_{j=1}^{n} a_{ij}\, S_j^* = N_i \qquad (i = 1, \ldots, n)\,. \tag{4.2.3}$$

The unfolded spectrum $\boldsymbol{S}^*$ has to be corrected for the photoelectrical efficiency $\varepsilon(E)$ of the detector in order to get the real γ-spectrum $\boldsymbol{S}$:

$$S_j = \frac{S_j^*}{\varepsilon(E_j)}\,. \tag{4.2.4}$$

We performed the unfolding (4.2.3) with 3 different methods: the inversion of the matrix $\boldsymbol{A}$, the iterative method of Gauss-Seidel [37] and the correction factor method of Scofield [38].

All these methods lead to the same result $\boldsymbol{S}^*$. As we had 300 points to unfold, we proceeded in steps of 100 points, starting from the right end of our spectrum. The left 10 points of each intermediate solution $\boldsymbol{S}^*$ oscillated [38, 39] and had to be suppressed. Therefore the next step started 10 channels more to the right.

After each step we subtracted from the unprocessed region the Compton contributions of the interval processed by this step. These contributions were computed by folding the solution $\boldsymbol{S}^*$ of this step with the matrix $\boldsymbol{A}$.

The final result $\boldsymbol{S}^*$ of this unfolding procedure may be seen in Figure 5.

We may remark that the correction of finite resolution is already executed by this unfolding as the approximation of the photopeaks in $\boldsymbol{A}$ is good enough (Fig. 8).

4.3 *The construction of the response matrix A*

According to (4.2.1), a function $\Phi(x, E)$ has to be found, which enables us to compute over the energy range of our IB measurement (300 keV $\leqslant x \leqslant$ 850 keV) single spectra produced in our γ-spectrometer (Ge(Li) detector) by photons of an arbitrary energy E (300 keV $\leqslant E \leqslant$ 850 keV). Then

$$a_{ij} = \Phi(x_i, E_j)\,. \tag{4.3.1}$$

As the shape of this single spectrum depends on the γ-energy, we introduce a set of M shaping parameters p_m which carry the E dependence of Φ.

$$\Phi(x, E) = \Phi(x; p_1, \ldots, p_m, \ldots, p_M) \tag{4.3.2}$$

where $p_m = p_m(E)$.

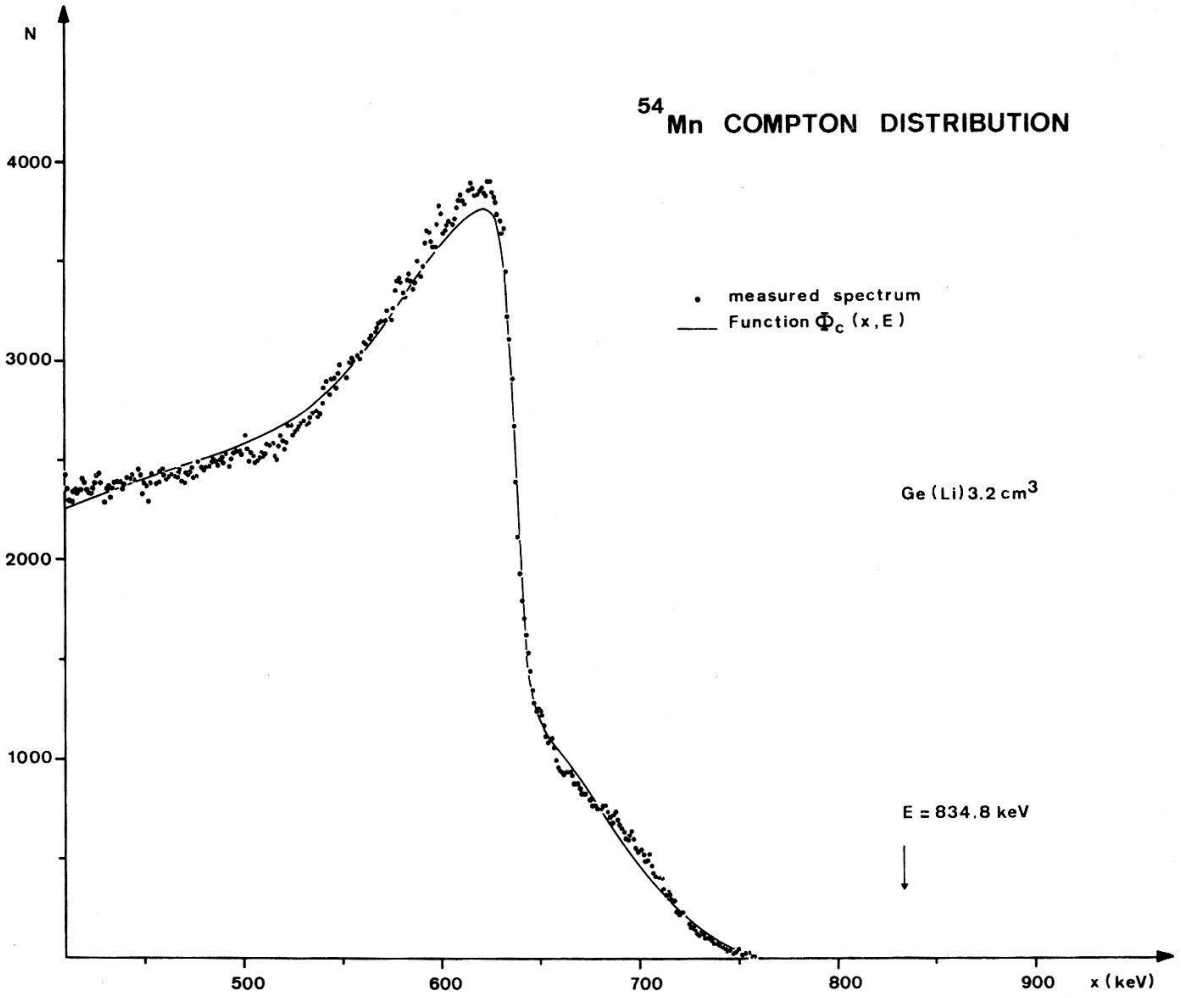

Figure 7
The function (4.3.4) adapted by a non linear least squares fit.

The following function Φ reproduced with good accuracy single Ge(Li) spectra:

$$\Phi(x; p_m) = \begin{cases} \Phi_c(x; p_1, \ldots, p_{10}) & \text{for } x \leqslant p_{18} \\ \Phi_p(x; p_{11}, \ldots, p_{17}) & \text{for } x > p_{18}\,. \end{cases} \tag{4.3.3}$$

Φ_c and Φ_p represent the Compton distribution respectively the photopeak. The detailed expressions are:

$$\left.\begin{aligned} &\Phi_c(x; p_1, \ldots, p_{10}) = \{\text{GROUND}\} + \{\text{STAIR}\} + \{\text{HILL}\} \\ &\text{where} \\ &\{\text{GROUND}\} = p_1 + p_2\, x + p_3\, x^2\,, \\ &\{\text{STAIR}\} = \frac{p_4}{1 + \exp\left((x - p_5)/p_6\right)}\,, \\ &\{\text{HILL}\} = p_7 \exp - \frac{1}{2}\left(\frac{x - p_8}{\Sigma}\right)^2 \\ &\text{and} \\ &\Sigma = \begin{cases} p_9 & \text{for } x \leqslant p_8 \\ p_{10} & \text{for } x > p_8\,. \end{cases} \end{aligned}\right\} \tag{4.3.4}$$

$$\left.\begin{aligned}
&\Phi_p(x; p_{11}, \ldots, p_{17}) = \frac{p_{11}}{p_{12}} [\{\text{GAUSS}\} \cdot \{\text{DEF}\} + \delta \cdot \{\text{TAIL}\} \cdot \{\text{MOD}\}] \\
&\text{where} \\
&\{\text{GAUSS}\} = \frac{1}{\sqrt{2\pi}} \exp - \frac{1}{2}\left(\frac{x - p_{13}}{p_{12}}\right)^2, \\
&\{\text{DEF}\} = 1 - \frac{2}{\pi} \tan^{-1} p_{14}\left(\frac{x - p_{13}}{p_{12}}\right), \\
&\{\text{TAIL}\} = p_{15} + p_{16} \exp p_{17}\left(\frac{x - p_{13}}{p_{12}}\right), \\
&\{\text{MOD}\} = 1 - \frac{1}{((x - p_{13})/p_{12})^2 + 1} \\
&\text{and} \\
&\delta = \begin{cases} 1 & \text{for } x \leqslant p_{13} \\ 0 & \text{for } x > p_{13}\,. \end{cases}
\end{aligned}\right\} \quad (4.3.5)$$

The terms STAIR (Fermi distribution function) and HILL (Asymetric Gaussian curve) reproduce the Compton-edge. The factor DEF accounts for the skewness of the photopeak, while MOD lessens the strength of the low energy tail in the neighbourhood of the peak centroid. A similar analytical expression to (4.3.5) was described extensively by Kern [21].

In order to specify the E dependence of the 18 parameters, we calibrated our γ-spectrometer with 6 single spectra of different γ-energies E: ^{203}Hg (279.2 keV), ^{51}Cr (320.0 keV), ^{198}Au (411.8 keV), ^{85}Sr (514.0 keV), ^{137}Cs (661.8 keV) and ^{54}Mn (834.8 keV).

With a non-linear least squares technique [40] we adapted the functions Φ_c and Φ_p to these measured spectra and recieved for each parameter p_m a set of experimental values f_{mj}:

$$p_m(E_j) = f_{mj}\,.$$

The result of this fit is shown in Figures 7 and 8 for $E = 834.8$ keV.

We interpolated each parameter p_m with a polynomial $P_m(E)$ adapted to the set of values f_{mj} by a linear least squares fit.

$$p_m(E) = P_m(E)\,. \quad (4.3.6)$$

The degrees of the polynomials lay within the range -4 to $+4$. Each $P_m(E)$ is given by its coefficients, so that 18 sets of coefficients enable us to compute the function Φ for any value of x and E taken in the calibrated energy range.

4.4 *Theoretical spectral shape and* JAUCH *plot*

Like for ordinary electron captures, the radiative capture of the $K, L, M, \ldots$ electrons occurs with different probabilities. According to Glauber [41] and Martin [42] the shape of the internal bremsstrahlung spectrum emitted during this process depends

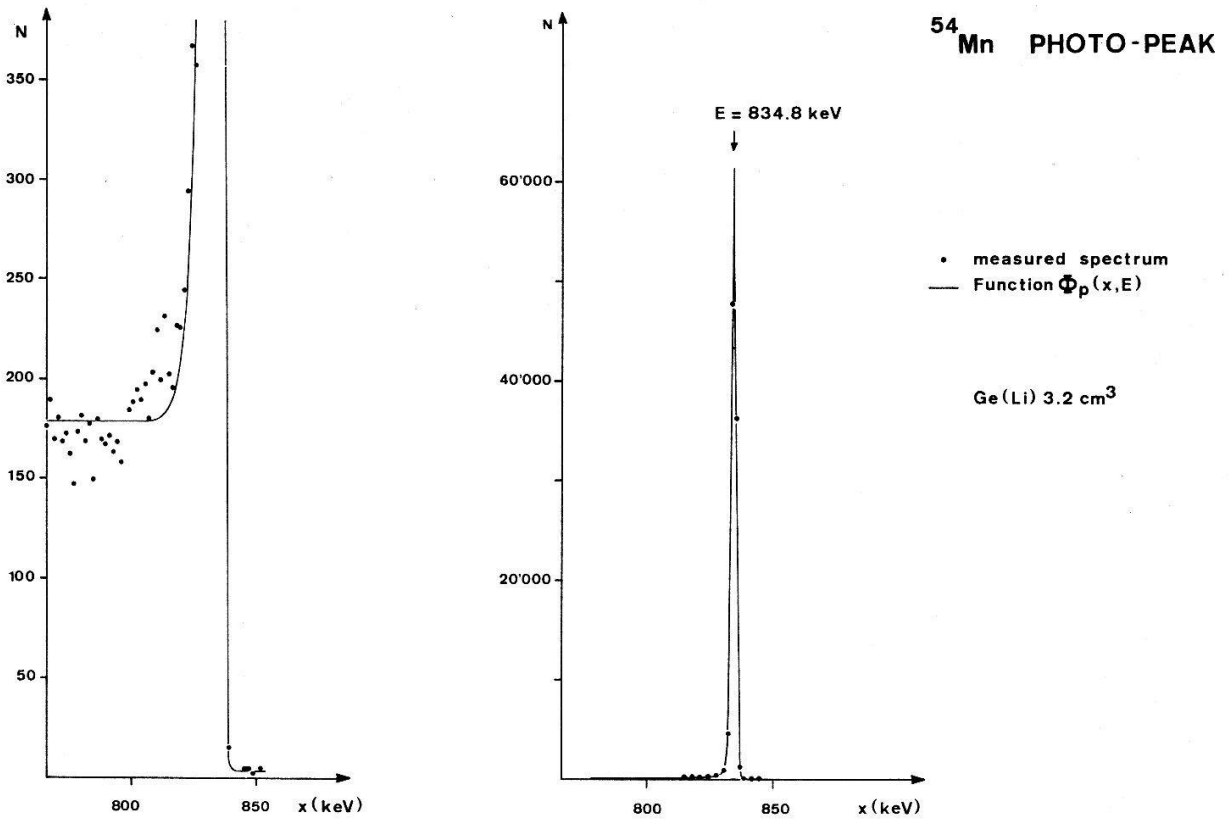

Figure 8
The function (4.3.5) adapted by a non linear least squares fit.

strongly on the angular momentum l of the captured electron, while the relative intensity decreases with the principal quantum number n.

Most of the radiated intensity is created by the capture of the s-electrons (s-spectra). The p-spectra are strongly dominant at low energies but are insignificant above $E = Z \alpha\, m\, c^2$ (Our case: $Z = 24$, $Z \alpha\, m\, c^2 = 90$ keV). The spectra for higher l values have never been treated theoretically. Their intensity may also be neglected above $E = Z \alpha\, m\, c^2$.

We consider only the high energy region of our experimental IB spectrum ($E > 600$ keV), which is assumed to be free from pile up distortion. This region contains only s-contribution. This latter assumption has been tested on the similar IB spectrum emitted by ^{49}V (Fig. 7 of [42]).

The shape of the ns-spectra has been computed by Glauber [41] using non relativistic electron wave functions:

$$\frac{dW_{ns}}{W_K} = \frac{\alpha}{\pi (m\, c^2)^2} \frac{1}{(E_F^{1s})^2} \left| \frac{\varphi_{ns}(0)}{\varphi_{1s}(0)} \right|^2 R_{ns}(E)\, E\, (E_F^{ns} - E)^2\, dE\,, \tag{4.4.1}$$

where

dW_{ns}	probability for an ns-electron to be captured with emission of IB in the energy range E, $E + dE$
W_K	total number of non-radiative K captures
E_F^{ns}	end point energy of the ns-spectrum
$\varphi_{ns}(0)$	screened radial wave function of the ns-electron taken in the nuclear vicinity

The relativistic factor $R_{ns}(E)$ varies slowly with E and approaches unity for energies lying far above the X-ray region. It takes into account the relativistic interaction of the magnetic moment of the ns-electron with the Coulomb field of the nucleus. This factor alters the spectral shape only at low energy ($E < 100$ keV) and weakens the intensity at higher energies. It is tabulated [41, 42].

The difference of the end point energies E_F^{1s} and E_F^{2s} equals the difference between the binding energies of the states 1s and 2s. For our case, this difference is 5.3 keV and is negligible compared to the accuracy (14 keV) of the end point energy (742 keV) (Fig. 9).

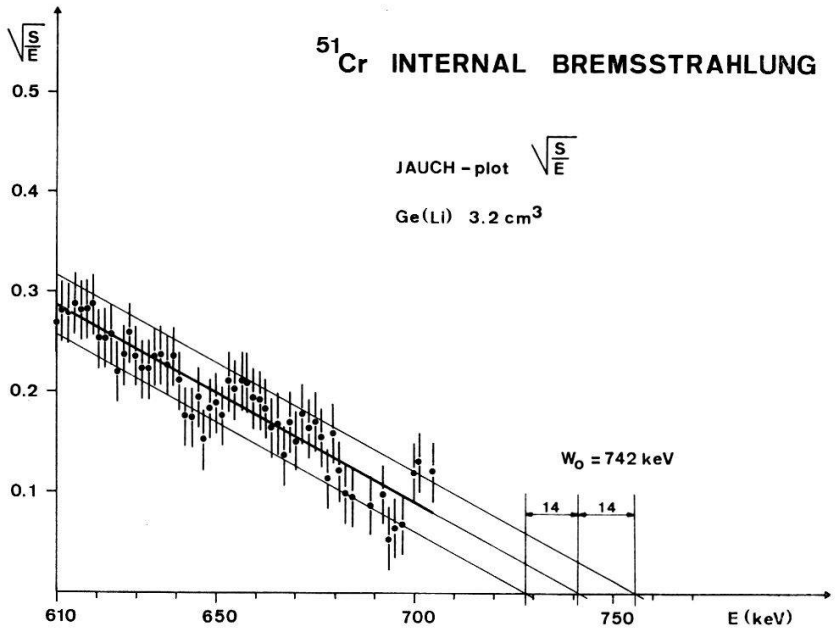

Figure 9
The determination of the end point energy W_0. The middle line was adapted to the experimental points by a weighted least squares fit. The higher and lower lines limit the $\pm\,\sigma$ range.

According to Glauber [41], we assume that $R_{1s}/R_{2s} \sim 1$. We can deduce from (4.4.1) the ratio of the 1s to the 2s-component. This ratio is approximately given by $|\varphi_{1s}(0)/\varphi_{2s}(0)|^2$. Using the electron wave function for pure Coulomb field [43] and correcting them with the appropriate screening factor (Fig. 3 of [42]), we get this amplitude ratio to 11.7.

As the 1s-component is dominant, the total IB spectrum has the shape $E\,(W_0 - E)^2$ where $W_0 = E_F^{1s}$. We may then adapt to the points S_j (Calculated from (4.2.4)) the spectral function

$$S(E) = S_0\,E\,(W_0 - E)^2\,,$$

where S_0 and W_0 are 2 parameters to be determined. W_0 is easily determined from the JAUCH plot $J(E)$:

$$J(E) = \sqrt{\frac{S}{E}} = S_0^{1/2}\,(W_0 - E)\,. \qquad (4.4.2)$$

The diagram $J(E)$ is a straight line. Figure 9 shows the experimental points and the straight line adapted with a weighted linear least squares fit.

We get:

$$W_0 = (742 \pm 14) \text{ keV}$$

and

$$Q = (W_0 + B_{1s})$$

$$\boxed{Q = (748 \pm 14) \text{ keV}}.$$

B_{1s} is the binding energy of the 1s-electron in ^{51}Cr: 5.989 keV. Our result agrees with the previous values (Table 4). Some of these were obtained with independent methods.

Table 4
Q value of the electron capture decay $^{51}\text{Cr} \rightarrow {}^{51}\text{V}$

Ref.	Method	Q (keV)
Richards [36]	$^{51}\text{V}(p, n)^{51}\text{Cr}$	750 ± 6
Bisi [1]	IB, NaI(Tl)	756 ± 5
Cohen [44]	IB, NaI(Tl)	780 ± 50
Ofer [2]	IB, NaI(Tl)	730 ± 20
Van der Kooi [45]	IB, NaI(Tl)	752 ± 22
Gosset [46]	$^{51}\text{V}(p, n)^{51}\text{Cr}$	751 ± 3
Gosset [46]	$^{50}\text{Cr}(n, \gamma)^{51}\text{Cr}$ $^{50}\text{Cr} - {}^{51}\text{V}$ mass sp	752 ± 13
Narasimhamurty [47]	IB, NaI(Tl)	778 ± 40
Present work	IB, Ge(Li)	748 ± 14

4.5 *Branching ratio of the electron capture*

The IB spectrum and the measurement of the 320 keV transition (Fig. 5) enables us to determine the fraction β of electron captures leading to the 1st excited state of ^{51}V (Fig. 10).

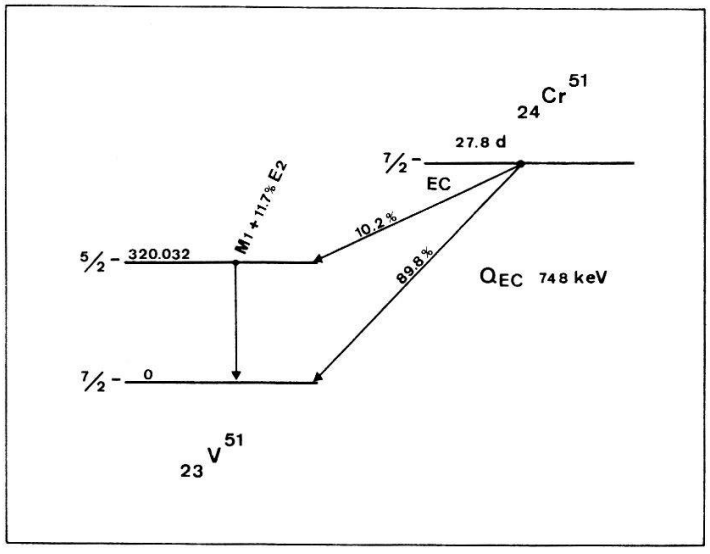

Figure 10
The proposed decay scheme of ^{51}Cr.

From the ratio of the intensity of the 320 keV γ-rays (N_γ) to the intensity of photons (N_{IB}) emitted in a certain spectral range ($\Delta E = E_2 - E_1$) by the ground-to-ground internal bremsstrahlung we have:

$$\frac{\beta}{1-\beta} = \frac{N_\gamma}{N_{IB}} W_{IB}\,, \tag{4.5.1}$$

where

$$W_{IB} = \int_{E_1}^{E_2} dW_{IB} = \frac{\alpha}{\pi} \int_{E_1}^{E_2} E\left(1 - \frac{E}{E_F}\right)^2 dE\,.$$

W_{IB} is the integrated probability of the IB-emission in the spectral range ΔE. It can be derived from (4.4.1) giving the energies in $m\,c^2$. The total internal conversion coefficient of the 320 keV transition has the magnitude 10^{-3} and therefore may be neglected.

We got by this method:

$$\boxed{\beta = (10.2 \pm 1)\,\%}\,.$$

The agreement with previous values is good (Table 5).

Table 5
The branching ratio β of the electron capture $^{51}\mathrm{Cr} \rightarrow {}^{51}\mathrm{V}$

Ref.	Method	Branching ratio (%)
Lyon [48]	X-γcoinc	8
Bunker [13]	X-γcoinc	(9.8 ± 0.6)
Cohen [44]	γ/IB ratio	7
Bisi [1]	γ/X ratio	9.8
Ofer [2]	γ/IB ratio	(9 ± 1)
Present work	γ/IB ratio	(10.2 ± 1)

4.6 *IB measurement with the magnetic spectrometer*

In order to test our IB spectrum taken with the Ge(Li) detector, we performed an independent measurement in external conversion (Uranium converter) with the above used magnetic spectrometer.

The response matrix $\boldsymbol{B}$ of the converter-spectrometer system was constructed according to (4.3). The Compton distributions were fitted by a polynomial of the 3rd degree. The function (4.3.5) with DEF $\equiv 1$ reproduced with good accuracy the different conversion lines, the relative intensities of which were expressed with further parameters.

Unfortunately the Compton contributions were no more small corrections to the K-conversion, so that the unfolding was impossible to be performed by iterative methods. The rank of $\boldsymbol{B}$ was too high to allow its inversion with the available computers.

Nevertheless we *folded* with the matrix B the real IB spectrum deduced from the Ge(Li) measurement and obtained a spectrum which can be compared to the measurement performed with the magnetic spectrometer. Both spectra agree qualitatively above $B\varrho = 2600$ Gauss cm. Below this $B\varrho$ value the magnetic spectrometer spectrum has a deformation which cannot be explained. In a Ge(Li) measurement, this deformation, if real, would be overwhelmed by the pile up effect.

5. Conclusion

The exclusion of the hypothetical transitions of (150), (325), (470) and (645) keV enables us to rearrange the decay scheme of ^{51}Cr. We propose in Figure 10 a decay scheme with our measured values.

The calculations of chapter 4 were coded in FORTRAN IV and performed with the computers IBM 7040 (Swiss Institute of Technology, Lausanne) and UNIVAC-III (Electronic Computation Center, University of Fribourg).

Acknowledgements

The authors are gratefully indebted to Prof. Dr. J. Kern, who initiated this work, for his help in computation problems and for the stimulative discussions. They acknowledge the useful comments from Prof. Dr. L. Schellenberg. We thank Dr. S. Hultberg[7]) for the computation of the f value necessary to the K-ICC determination. We are grateful to dipl. el. ing. L. Ribordy for the electronic improvements on the spectrometer control and to Mr. H. Tschopp for the careful maintenance of this instrument. The assistance of B. Michaud, G. Mauron and D. Geinoz during the measurements and the help of Miss M. Rossier in the preparation of data are here acknowledged.

C. R. wishes especially to thank IBM International Business Machines (Extension Suisse) for 15 free hours on the IBM 7040 computer of the Swiss Institute of Technology in Lausanne.

REFERENCES

[1] A. Bisi, E. Germagnoli and L. Zappa, Nuov. cim. *2*, 1052 (1955).
[2] S. Ofer and R. Wiener, Phys. Rev. *107*, 1639 (1957).
[3] Gy. Mathé, Nucl. Phys. *46*, 236 (1963).
[4] I. Talmi, in Proc. of the Rehovoth Conf. on Nuclear Structure (North-Holland Publishing, Amsterdam 1958), p. 31.
[5] J. D. Mc Cullen, B. F. Bayman and L. Zamick, Phys. Rev. *134*, B515 (1964).
[6] J. E. Schwäger, Phys. Rev. *121*, 569 (1961).
[7] W. Scholz and F. B. Malik, Phys. Rev. *147*, 836 (1966).
[8] T. Y. Chen, O. Huber, J. Kern, L. Schellenberg, B. Walthard and H. Wild, Nucl. Instrum. Meth. *29*, 181 (1964).
[9] J. Kern, Cl. Ribordy and O. Huber, Helv. phys. Acta *36*, 820 (1963).
[10] Cl. Ribordy, O. Huber, P. Siffert and L. Stab, Helv. phys. Acta *39*, 262 (1966).
[11] A. F. Kluk, private communication of J. H. Hamilton quoted in [12]. D. Krmpotic, A. F. Kluk and J. H. Hamilton, Bull. Am. Phys. Soc. *13*, 1723 (1968), JC7.
[12] J. C. Hill, Nucl. Phys. *A136*, 564 (1969).

[7]) Research Institute for Physics, Stockholm 50.

[13] M. E. Bunker and J. W. Starner, Phys. Rev. *97*, 1272 (1955).
[14] G. Murray, R. L. Graham and J. S. Geiger, Nucl. Phys. *63*, 353 (1965).
[15] G. T. Ewan, A. J. Tavendale, Can. J. Phys. *42*, 2286 (1964).
[16] R. L. Robinson, P. H. Stelson, F. M. Mc Gowan, J. L. C. Ford jr. and W. T. Milner, Nucl. Phys. *74*, 281 (1965).
[17] W. R. Pierson, Phys. Rev. *140*, B1516 (1965).
[18] D. H. White, B. G. Saunders, W. Johns and R. J. Jewell, Nucl. Phys. *72*, 241 (1965).
[19] W. W. Black and R. L. Heath, Nucl. Phys. *A 90*, 650 (1967).
[20] J. J. Reidy quoted in Nucl. Instrum. Meth. *57*, 219 (1967).
[21] J. Kern, Nucl. Instrum. Meth. *79*, 233 (1970).
[22] H. W. Baer, J. J. Reidy and M. L. Wiedenbeck, Nucl. Phys. *A 113*, 33 (1968).
[23] R. Gunnink, R. A. Meyer, J. B. Niday and R. P. Anderson, Nucl. Instrum. Meth. *65*, 26 (1968).
[24] S. Hultberg and R. Stockendal, Arkiv Fysik *14*, 565 (1959).
[25] S. Hultberg, Arkiv Fysik *15*, 307 (1959).
[26] S. Hultberg and P. Erman, Arkiv Fysik *37*, 151 (1968).
[27] S. Hultberg, B. Nagel and P. Olsson, Arkiv Fysik *38*, 1 (1968).
[28] O. Dragoun, Cl. Ribordy and O. Huber, Nucl. Phys. *A 124*, 337 (1969).
[29] M. E. Rose, Internal Conversion Coefficients (North-Holland Publ. Co., Amsterdam 1958).
[30] D. Maeder, P. Preiswerk and A. Steinemann, Helv. phys. Acta *25*, 461 (1952).
[31] M. E. Bunker and J. W. Starner, Phys. Rev. *99*, 1906 (1955).
[32] I. V. Estulin and E. M. Moiseeva, JETP *28*, 541 (1955).
[33] Z. O'Friel and A. H. Weber, Phys. Rev. *101*, 1076 (1956).
[34] Z. O'Friel and A. H. Weber, Phys. Rev. *99*, 659 (1955).
[35] U. C. Gupta, M. G. Shahani and P. K. Srivastava, J. Sci. Industr. Res. *21 B*, 1 (1962).
[36] H. T. Richards, R. V. Smith and C. P. Browne, Phys. Rev. *80*, 524 (1950).
[37] R. Zurmühl, *Praktische Mathematik für Ingenieure und Physiker* (Springer Verlag, Berlin, Heidelberg und New York 1965), p. 157.
[38] N. E. Scofield, in *Applications of Computers to Nuclear and Radiochemistry*. Proc. Symp. of Gatlinburg 1962, ed. by G. D. O'Kelley (USAEC, NAS-NS3107), p. 108.
[39] W. Kreische, W. Lampert and G. Loos, Nucl. Instrum. Meth. *42*, 188 (1966).
[40] J. Kern, *ISABELLE, a FORTRAN Non-linear Least Squares Fit Code*, University of Fribourg Report (1970).
[41] R. J. Glauber and P. C. Martin, Phys. Rev. *104*, 158 (1956).
[42] P. C. Martin and R. J. Glauber, Phys. Rev. *109*, 1307 (1958).
[43] H. A. Bethe and E. E. Salpeter, in *Encyclopedia of Physics*, Vol. *35*, ed. by S. Flügge (Springer Verlag, Berlin 1957), p. 88.
[44] S. G. Cohen and S. Ofer, Phys. Rev. *100*, 856 (1955).
[45] J. B. van der Kooi and H. J. van den Bold, Physica *22*, 681 (1956).
[46] C. R. Gosset and J. W. Butler, Phys. Rev. *113*, 246 (1959).
[47] K. Narasimhamurty and S. Jnanananda, *Atomic Energy Establishment Trombay (India)*, Report Nr. *267*, 68 (1966).
[48] W. S. Lyon, Phys. Rev. *87*, 1126 (1952).